Magnetic properties of $NpNiSi_2$

2008 J. Phys.: Condens. Matter 20 075207

(http://iopscience.iop.org/0953-8984/20/7/075207)

IOP PUBLISHING JOURNAL OF PHYSICS: CONDENSED MATTER

J. Phys.: Condens. Matter **20** (2008) 075207 (6pp) doi:10.1088/0953-8984/20/7/075207

Magnetic properties of $NpNiSi_2$

E Colineau[1,3], F Wastin[1], J P Sanchez[1,2] and J Rebizant[1]

[1] European Commission, Joint Research Centre, Institute for Transuranium Elements, Postfach 2340, D-76125 Karlsruhe, Germany

[2] CEA, Département de Recherche Fondamentale sur la Matière Condensée, 38054 Grenoble cedex 9, France

E-mail: eric.colineau@ec.europa.eu

Received 8 November 2007, in final form 20 December 2007
Published 25 January 2008
Online at stacks.iop.org/JPhysCM/20/075207

Abstract

$NpNiSi_2$ represents the first transuranium-based system in the isostructural family with rare earths and uranium homologues that crystallizes into the orthorhombic *Cmcm* structure. It exhibits strong anisotropic ferromagnetic ordering below $T_C = 51.5$ K with the easy magnetization axis along the shortest (*c*) axis. The ordered magnetic moment inferred from ^{237}Np Mössbauer spectroscopy amounts to $\mu_{Np} = 1.4\ \mu_B$. The isomer shift value of 6.8 mm s^{-1} versus $NpAl_2$ suggests that the neptunium ions are in the Np^{3+} charge state with electronic configuration $5f^4$ ($J = 4$). From the values of the quadrupolar interaction parameters, the direction of the main principal axis of the electric field gradient (V_{ZZ}) is deduced to be along the *b* axis. The Sommerfeld coefficient $\gamma = 133$ mJ mol^{-1} K^{-2} obtained from the low temperature behaviour of specific heat qualifies $NpNiSi_2$ as a moderately heavy fermion. Finally, the logarithmic decrease of the high temperature resistivity and the reduced (compared to the free Np^{3+} ion) magnetic moments (both ordered and effective) point to the occurrence of a Kondo effect. $NpNiSi_2$ hence appears as a good candidate for being described with the underscreened Kondo lattice model of Perkins *et al* (2007 *Phys. Rev.* B **76** 125101) which accounts for the coexistence of the Kondo effect and ferromagnetic order.

1. Introduction

The study of isostructural families provides valuable information that allows identifying trends and key parameters that clarify general mechanisms driving the physical properties of intermetallic compounds. During the last decade, extensive studies have been performed in particular on the ternary series AnTX [1], AnT_2X_2 [1] and An_2T_2X [2] compounds (where An is an actinide, T a transition metal and X belongs to column IV). On the contrary, very few data exist on the $AnTX_2$ system that crystallizes in the orthorhombic *Cmcm* (no. 63) structure.

$RNiSi_2$ with light rare earths (R = Pr, Nd) [3] exhibit ferromagnetic ordering whereas those with heavy rare earths (R = Tb, Dy, Ho, Er) [4–7] show different types of uniaxial antiferromagnetic order. The magnetic moments point along the shortest (*c*) axis in all these compounds except in $ErNiSi_2$ [7] where the moment is oriented along the *b* axis. This points out that the magnetocrystalline anisotropy in the $RNiSi_2$ compounds is crystal field induced and that the lowest order anisotropy constant is determined by the sign of the second order Stevens factor (negative for Pr, Nd, Tb, Dy and Ho and positive for Er). It is also worth mentioning that $CeNiSi_2$ [8] as well as $EuNiSi_2$ [9] exhibit intermediate valence and spin fluctuations are clearly evidenced in the Ce compound. The uranium compounds $UTSi_2$ (with T a 3d transition metal) [10] show a clear trend of increasing 5f localization (corresponding to decreasing 5f–3d hybridization) along the series: whereas $UFeSi_2$ is a weakly temperature dependent paramagnet and $UCoSi_2$ a spin fluctuation system, $UNiSi_2$ is a ferromagnetically ordered ($T_C = 95$ K) Kondo lattice with rather well-localized 5f electrons [10]. The 1.2 μ_B U moments are directed along the *c* axis [11]. The specific heat Sommerfeld coefficient amounts to $\gamma = 21$ mJ mol^{-1} K^{-2} [12]. It should also be mentioned that $UPtSi_2$ was reported to be a ferromagnet with $T_C \sim 86$ K [13].

In order to extend these investigations to transuranium systems, we have undertaken the study of $NpNiSi_2$ and present here the first results on this system, obtained by magnetization, electrical resistivity, specific heat and ^{237}Np Mössbauer spectroscopy.

[3] Author to whom any correspondence should be addressed.

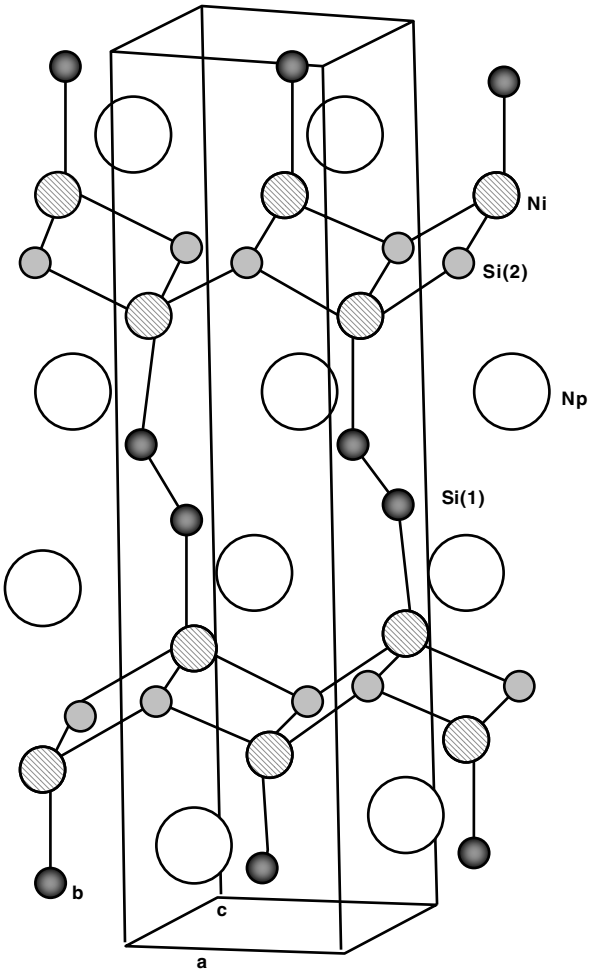

Figure 1. Crystallographic structure of $NpNiSi_2$.

2. Experimental details

Single crystals of $NpNiSi_2$ were grown by the Ga flux method and characterized by x-ray diffraction. The intensities collected on an Enraf-Nonius CAD-4 four circle diffractometer using a monochromatic Mo Kα_1 radiation were corrected for Lorentz and polarization effects, and an absorption correction was applied using the psi-scans method. Examination of the systematic extinction confirmed that $NpNiSi_2$ crystallizes in the orthorhombic structure with space group $Cmcm$ ($CeNiSi_2$ type) [14, 15]. The refined structural parameters are $a = 4.0207(7)$ Å, $b = 16.1253(35)$ Å, $c = 3.9991(7)$ Å and the atomic positions are listed in table 1. The crystal structure is schematically shown in figure 1. It consists of layers perpendicular to the b axis with the following sequence Np–Ni–Si–Ni–Np–Si–Si–Np–Ni–Si–Ni–Np. The coordination around Np (site symmetry $m2m$) consists of 21 atoms, if bonding interactions are considered for distances <4.1 Å, resulting in a ($NpSi_4Ni_4Si_6NiNp_6$) polyhedron.

The shortest inter-neptunium spacing amounts to 3.913 Å, i.e. well above the Hill limit (≈3.2 Å for neptunium-based compounds) [16] whereas the shortest Np–Ni and Np–Si distances are 3.080 and 3.026 Å, respectively.

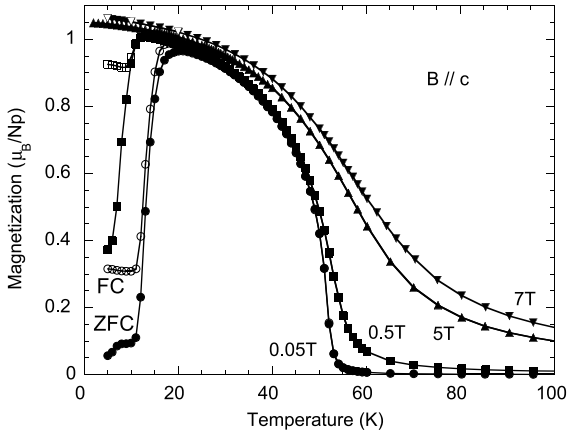

Figure 2. Zero-field cooled (ZFC) and field cooled (FC) magnetization of $NpNiSi_2$ in various fields ($B \parallel c$).

Table 1. Atomic positions of $NpNiSi_2$.

Atom	x	y	z
Np (4c)	0	0.104 28	1/4
Ni (4c)	0	0.321 14	1/4
Si1 (4c)	0	0.461 29	1/4
Si2 (4c)	0	0.750 29	1/4

DC magnetization measurements were carried out on a Quantum Design SQUID magnetometer (MPMS-7) in magnetic fields up to 7 T on 5.90 and 4.33 mg single crystals for $B \parallel c$ and $B \parallel b$, respectively. The electrical resistivity was measured in a Quantum Design PPMS-9 system by an AC four-probe technique on a ∼2 × 1 × 1 mm^3 sample, and in applied fields up to 9 T ($B \parallel c$). The specific heat experiments were performed using 3.83 and 30.53 mg single crystals for $B \parallel c$ and $B \parallel b$, respectively, by the relaxation method in the PPMS-9 within the temperature range 4.2–300 K and in magnetic fields up to 9 T. The ^{237}Np Mössbauer spectra were recorded using a sinusoidal drive motion of a ^{241}Am metal source kept at 4.2 K. The temperature of the absorber containing 162 mg Np cm^{-2} was varied from 4.2 to 60 K. The velocity scale of the spectrometer was calibrated with reference to an $NpAl_2$ absorber ($B_{hf} = 330$ T at 4.2 K).

3. Results

3.1. Magnetization

The magnetization recorded at $B = 0.05$ T as a function of temperature clearly shows the onset of ferromagnetic order in $NpNiSi_2$ below $T_C = 51.5$ K (figure 2) as determined by the $dM(T)/dT$ derivative. A sharp collapse of the magnetization is observed at $T^* \approx 12$ K, most likely due to domain effects. However, the possible occurrence of an antiferromagnetic transition at T^* cannot, at this stage, be ruled out. The sharp magnetization collapse at T^* observed both on zero-field cooled (ZFC) and field cooled (FC) curves at low fields, weakens when the field increases and finally vanishes above 1 T. At high fields, both ZFC and FC curves

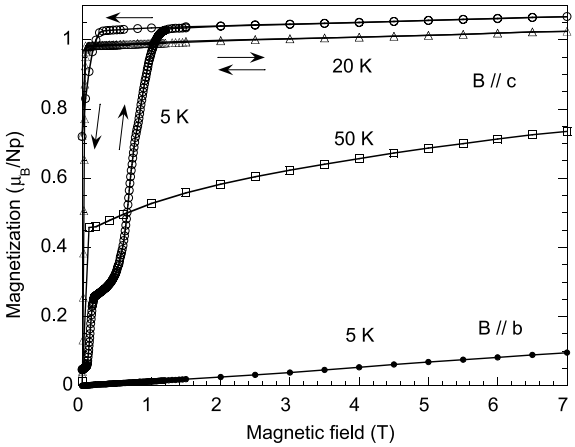

Figure 3. Magnetization curves of $NpNiSi_2$ versus magnetic field ($B \parallel c$) at various temperatures and at $T = 5$ K for $B \parallel b$. The arrows indicate the cycle of measurements.

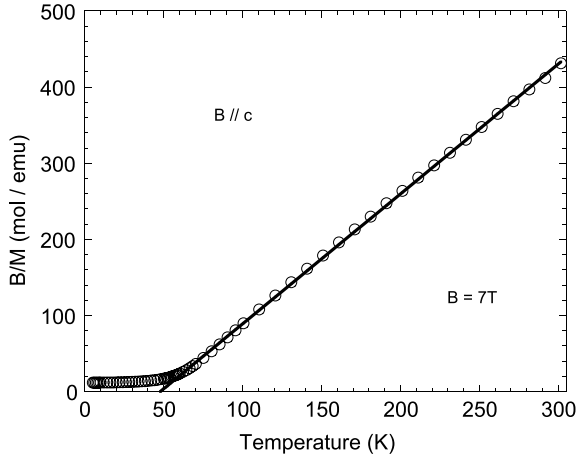

Figure 4. Inverse magnetic susceptibility (open circles) of $NpNiSi_2$ recorded in 7 T ($B \parallel c$) and Curie–Weiss fit (solid line).

superpose and converge to $\mu_{sat} \approx 1.07\ \mu_B$. The saturated moment can be also observed on the magnetization plotted versus magnetic field (figure 3) for different temperatures. It should be noticed that below T^*, as illustrated on the 5 K curve, the saturation is reached in two steps. These jumps occur below 1 T, consistently with the $M(T)$ curves discussed above.

So far, only magnetization curves with magnetic field applied along the c axis were discussed. Measurements with the magnetic field applied perpendicular to the c axis ($B \parallel b$) reveal a strong magnetic anisotropy (figure 3): no saturation is observed and the magnetization at 5 K and 7 T is smaller by one order of magnitude than along the c axis.

In the paramagnetic state, the magnetic susceptibility $\chi(T)$ of $NpNiSi_2$ obeys a Curie–Weiss law (figure 4) that yields a paramagnetic Curie temperature $\theta_p \approx 48$ K quite close to the Curie temperature $T_C \approx 51.5$ K and an effective magnetic moment $\mu_{eff} = 2.16\ \mu_B$, lower than the free ion values (2.75 and 3.68 μ_B in the intermediate coupling scheme for Np^{3+} and Np^{4+}, respectively).

3.2. Electrical resistivity

The electrical resistivity (figure 5) confirms the onset of magnetic order at 51.5 K, but also the presence of a second anomaly around 13 K, close to T^*. This slight anomaly is very field sensitive and vanishes when magnetic fields (>0.3 T) are applied. This anomaly might be due to the existence of a low temperature antiferromagnetic phase, easily destroyed (to induced ferromagnetism) with the application of an external magnetic field but needs confirmation (see next section). The negative magnetoresistance in the whole temperature range (figure 5) would be compatible with a ferromagnet with magnetic domains [17].

The low temperature part of the resistivity (figure 5) can be reproduced by a simple T-square law below ~8 K:

$$\rho(T) = \rho_0 + aT^2$$

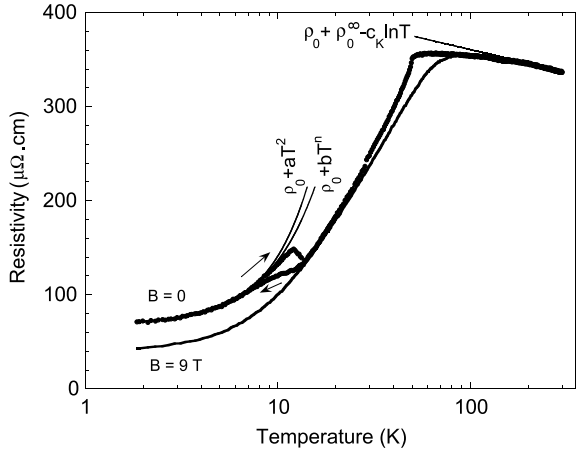

Figure 5. Electrical resistivity of $NpNiSi_2$ in zero field and with $B = 9$ T. Arrows indicate the direction of temperature variation. Solid lines show low and high temperature fits.

with $\rho_0 = 69.4\ \mu\Omega$ cm the residual resistivity and $a = 0.72\ \mu\Omega$ cm K^{-2}.

From the Kadowaki–Woods ratio $a/\gamma^2 \sim 10^{-5}\mu\Omega$ cm mJ^{-2} mol^2 K^2 [18], a rough estimate of the Sommerfeld coefficient, $\gamma \sim 268$ mJ mol^{-1} K^{-2}, can be inferred. It should be mentioned that if the temperature exponent is let free in the fit $\rho - \rho_0 = bT^n$, it converges to $n \sim 1.7$, i.e., close to 5/3, which could indicate the presence of ferromagnetic spin fluctuations.

Above the Curie temperature, the resistivity of $NpNiSi_2$ decreases logarithmically (figure 5). and can be accounted for by the Kondo-like formula

$$\rho(T) = \rho_0 + \rho_0^{\infty} - c_K \ln T$$

with $\rho_0 = 69.4\ \mu\Omega$ cm the residual resistivity as inferred from the low temperature fit, $\rho_0^{\infty} = 389\ \mu\Omega$ cm the temperature independent spin disorder term and $c_K = 20.9\ \mu\Omega$ cm the Kondo coefficient.

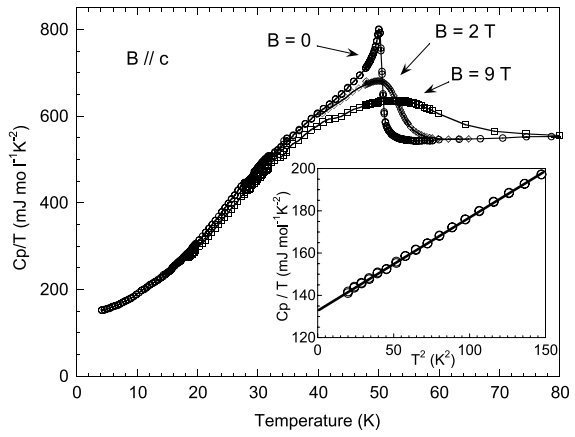

Figure 6. Specific heat of $NpNiSi_2$ at various fields applied parallel to the c axis.

3.3. Specific heat

The specific heat (figure 6) exhibits a clear lambda-type transition at $T_C = 51.5$ K, in excellent agreement with the other techniques. Applying magnetic field along the c direction broadens the peak and shifts entropy to higher temperatures. Such behaviour is typical for ferromagnetic ordering. No anomaly is observed at lower temperature, ruling out any further transition and indicating that the features observed at T^* by magnetization and resistivity measurements could be due to domain effects.

In the low temperature range (4.2–12 K), the specific heat can be reproduced by a simple law accounting for electronic and phononic contributions (figure 6—inset):

$$Cp/T = \gamma + \beta T^2.$$

The Sommerfeld coefficient amounts to $\gamma \approx 133$ mJ mol^{-1} K^{-2}, which qualifies $NpNiSi_2$ as a moderate heavy fermion system. Additionally, the Debye temperature can be estimated to $\theta_D \approx 164$ K, from $\beta = 0.438$ mJ mol^{-1} K^{-4} through the relation $\beta = \frac{12\pi^4}{5}\frac{R}{\theta_D^3}$ where R is the molar gas constant.

3.4. ^{237}Np Mössbauer spectroscopy

Figure 7 shows ^{237}Np Mössbauer spectra recorded at different temperatures between 4.2 and 60 K. At the latter temperature, i.e. in the paramagnetic state, the spectrum exhibits partial hyperfine splitting due to the quadrupolar interaction ($|eQV_{ZZ}| \approx 23.2$ mm s^{-1}). The asymmetry parameter is found to be $\eta = |(V_{XX} - V_{YY})/V_{ZZ}| \approx 0.24$. The position of the central line indicates an isomer shift $\delta_{IS} \approx 6.8$ mm s^{-1} versus the standard absorber $NpAl_2$. This suggests the occurrence of Np^{3+} charge state, corresponding to a $5f^4$ ($J = 4$) electronic configuration [19]. Fitting the spectra with these parameters (no magnetic hyperfine splitting), and plotting the line width as a function of temperature allows us to determine the ordering temperature $T_C \approx 51.5$ K. Below this temperature, the spectrum is further split by the magnetic hyperfine field that completely raises the degeneracy of the 5/2 ground and excited state nuclear levels (figure 7). Let aside

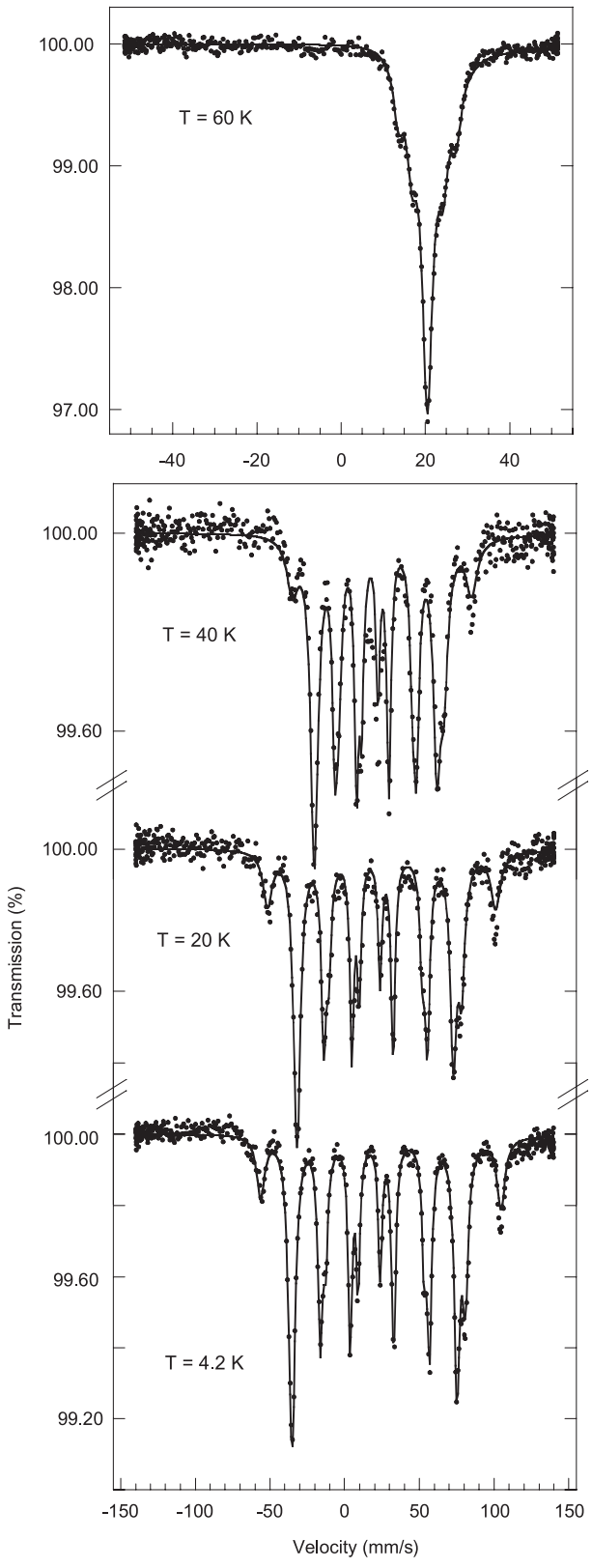

Figure 7. ^{237}Np Mössbauer spectra of $NpNiSi_2$ recorded at typical temperatures between $T = 4.2$ and 60 K.

increasing splitting and relaxation effects observed in a certain range below T_C, no particular change of the pattern is observed when decreasing temperature down to 4.2 K. This confirms

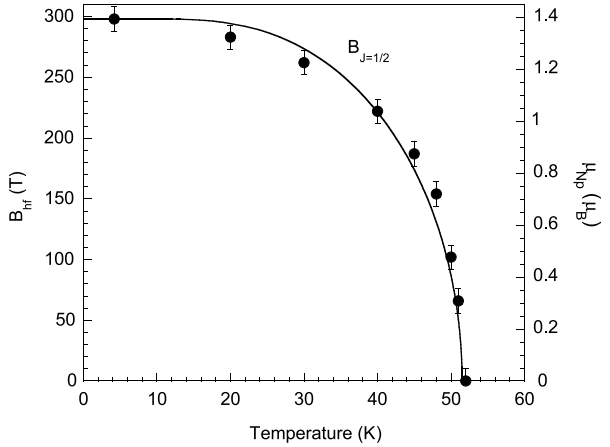

Figure 8. Thermal dependence of the ordered magnetic moment (right axis) of $NpNiSi_2$ as determined from the magnetic hyperfine field (left axis). The solid line represents a Brillouin function with $J = 1/2$.

the absence of any second transition, as shown by specific heat. In the ordered state, the effective quadrupolar interaction parameter $(eQV_{ZZ})_{\text{eff}}$ amounts to ≈ -13.0 mm s^{-1}, i.e. about half of the absolute value observed in the paramagnetic state. At 4.2 K, the well resolved spectrum yields an hyperfine magnetic field $B_{\text{hf}} \approx 298$ T, which corresponds to an ordered magnetic moment $\mu_{\text{Np}} = 1.4\ \mu_{\text{B}}$ carried by the neptunium atoms [20]. The thermal dependence of this magnetic moment is plotted on figure 8. It follows a $J = 1/2$ Brillouin behaviour which indicates that the ground state is a doublet.

The quadrupolar interaction parameter measured in the ordered state $(eQV_{ZZ})_{\text{eff}}$ is a projection onto the direction of B_{hf} of the quadrupolar interaction parameter $|eQV_{ZZ}|$ measured in the paramagnetic state according to the formula:

$$(eQV_{ZZ})_{\text{eff}} = (eQV_{ZZ}/2)(3\cos^2\theta - 1 + \eta \sin^2\theta \cos 2\varphi)$$

where θ and φ are the angles defining the orientation of B_{hf} (i.e. of the Np moments) in the electric field gradient (EFG) tensor reference axes. As the point symmetry of the neptunium ions is $m2m$, the principal axes of the EFG tensor coincide with the crystallographic axes. However, it is not possible to know *a priori* which crystallographic axis is the z axis of the EFG.

Assuming $\theta = 0°$ would lead to $(eQV_{ZZ})_{\text{eff}} = eQV_{ZZ}$, which does not correspond to the experimental observation, it is then justified to assume $\theta = 90°$.

Assuming $\varphi = 0°$ and 90°, we obtain $(eQV_{ZZ})_{\text{eff}} = -8.8$ mm s^{-1} and $(eQV_{ZZ})_{\text{eff}} = -14.4$ mm s^{-1}, respectively. The comparison with the experimental value $(eQV_{ZZ})_{\text{eff}} \approx -13.0$ mm s^{-1} then finally suggests that $\theta = \varphi = 90°$ and that eQV_{ZZ} is positive. From magnetization measurements we know that c is the easy axis and hence infer that $V_{ZZ} \parallel b$, $V_{YY} \parallel c$ and $V_{XX} \parallel a$.

All important parameters inferred from this Mössbauer study are listed in table 2.

Table 2. Main parameters inferred from Mössbauer experiments on $NpNiSi_2$ (see text).

δ_{IS} (mm s^{-1} versus $NpAl_2$)	6.8
$\lvert eQV_{ZZ}\rvert$ (mm s^{-1})	23.2
$(eQV_{ZZ})_{\text{eff}}$ (mm s^{-1})	−13.0
η	0.24
B_{hf} (T)	298
T_{C} (K)	51.5
θ	90°
φ	90°
$V_{ZZ} \parallel b$, $V_{YY} \parallel c$ and $V_{XX} \parallel a$	

4. Discussion

The different techniques used to investigate the physical properties of $NpNiSi_2$ are in agreement for the occurrence of ferromagnetic ordering below $T_{\text{C}} \approx 51.5$ K. They are also complementary and show that a difference exists between the ordered magnetic moment carried by neptunium ions and the saturated moment exhibited at the macroscopic scale (see table 3). This discrepancy is most probably due to the polarization of conduction electrons, resulting in a negative contribution to the total magnetization, although other more hypothetical explanations like complex ordering (small antiferromagnetic component, angle between magnetic moments and c axis) or slight experimental misalignment of the sample in magnetization experiments cannot be excluded at this stage.

Considering absolute values, both the ordered and effective magnetic moments are strongly reduced compared to the free ion Np^{3+} values (table 3). This is unlikely to be due to direct 5f–5f hybridization as the nearest Np–Np distance in $NpNiSi_2$ (≈ 3.913 Å) is well above the Hill limit (~3.2 Å for Np). On the contrary, the reduction of the magnetic moment is, besides crystal field effects, likely to originate from Kondo effect, which is strongly supported by resistivity data.

The values of the Curie temperatures of $UNiSi_2$ and $NpNiSi_2$ do not scale with the de Gennes factor $(G = (g_J - 1)^2 J(J+1))$ calculated for the free ions U^{3+} ($J = 9/2$, $g_J = 0.740$, $G = 1.673$) and Np^{3+} ($J = 4$, $g_J = 0.616$, $G = 2.949$) in the intermediate coupling scheme. This fact suggests that the Ruderman–Kittel–Kasuya–Yosida (RKKY) interaction alone is not sufficient to account for the magnetic interactions in the $AnNiSi_2$ system. The same remark applies too for the $RNiSi_2$ family [21]. As many other intermetallic compounds, $NpNiSi_2$ presents a huge magnetic anisotropy. Contrary to the rare earth $RNiSi_2$ analogues, its origin cannot be attributed to crystal field effects. Indeed, the second order Stevens factor for Np^{3+} ions is positive [22] as for Er^{3+} thus, the Np moments should align along the b axis and not point in the basal plane (c axis) as found experimentally. It is suggested that the direction of the Np moments is determined by bonding geometry. The Np ions are coordinated to four Ni nearest neighbours at 3.08 Å located in a plane perpendicular to the b axis. The hybridization of the 5f state of Np with the 3d state of Ni is a possible source of the rigid orientation of magnetic moment along the c axis.

Table 3. Properties of $UNiSi_2$ and $NpNiSi_2$.

	$UNiSi_2$ [10]	$NpNiSi_2$
a (Å)	4.028	4.0207
b (Å)	16.141	16.1253
c (Å)	4.027	3.9991
Unit cell volume (Å^3)	261.8	259.28
T_C (K)	96	51.5
θ_P (K)	95	48
μ_{ord} (μ_B) (free An^{3+} ion)	1.2 [11] (3.33)	1.4 (2.46)
μ_{sat} (μ_B)	1.12	1.07
μ_{eff} (μ_B) (free An^{3+} ion)	2.03 (3.68)	2.16 (2.75)
γ (mJ mol^{-1} K^{-2})	27 [12]	133
ρ_0 ($\mu\Omega$ cm)	15	69
ρ_0^∞ ($\mu\Omega$ cm)	399	389
c_K ($\mu\Omega$ cm)	28	21

Perkins *et al* [23] have recently developed an underscreened Kondo lattice model considering intra-site Kondo interaction and ferromagnetic inter-site interaction resulting from both RKKY interaction and direct exchange. This model appears to provide a good qualitative description of the unconventional properties of the uranium-based ferromagnetic compounds like UTe, $UCu_{0.9}Sb_2$ and $UCo_{0.5}Sb_2$ and coexistence of ferromagnetism and Kondo or heavy fermion behaviour. This model may well account for the properties of $UNiSi_2$ and $NpNiSi_2$.

Finally it can be mentioned that from the Kondo (c_K) and Sommerfeld (γ) coefficients listed in table 3, it can be seen that the Kondo character is less pronounced in $NpNiSi_2$ than in $UNiSi_2$, whereas the heavy fermion character is clearly stronger.

5. Conclusion

$NpNiSi_2$, the first transuranium compound of its series, was investigated by macroscopic and microscopic techniques. Ferromagnetic ordering develops below $T_C = 51.5$ K with easy axis along the shortest (c) axis. The saturated moment amounts to $\mu_{sat} = 1.07\ \mu_B$ at 5 K, whereas the ordered magnetic moment inferred from ^{237}Np Mössbauer spectroscopy is slightly larger, $\mu_{Np} = 1.4\ \mu_B$. This may be explained by the polarization of conduction electron and/or possible canting of the ferromagnetic order. The isomer shift amounts to 6.8 mm s^{-1} versus $NpAl_2$, indicating that neptunium ions are in the Np^{3+} charge state with electronic configuration $5f^4$ ($J = 4$). From the values of the quadrupolar interaction parameters, the direction of the main principal axis of the electric field gradient (V_{ZZ}), which is not known from the orthorhombic symmetry of the crystal, is deduced to be along the longest (b) axis. The Sommerfeld coefficient $\gamma = 133$ mJ mol^{-1} K^{-2} obtained by the low temperature behaviour of the specific heat qualifies $NpNiSi_2$ as a moderate heavy fermion. Comparison with the uranium homologue $UNiSi_2$ reveals large analogies and suggests that $NpNiSi_2$ is a rather localized 5f system.

Finally, the logarithmic decrease of high temperature resistivity and the reduced (compared to the free Np^{3+} ion) magnetic moments (both ordered and effective) point to the occurrence of the Kondo effect. $NpNiSi_2$ hence appears as a good candidate for the underscreened Kondo lattice model of Perkins *et al* [23] accounting for uranium heavy fermion systems with coexistence of ferromagnetism and the Kondo effect.

Acknowledgments

The authors are grateful to D Kakzorowski and B Coqblin for fruitful discussions. The high purity Np metals required for the fabrication of the compound were made available through a loan agreement between Lawrence Livermore National Laboratory and ITU, in the frame of a collaboration involving LLNL, Los Alamos National Laboratory and the US Department of Energy.

References

[1] Sechovsky V and Havela L 1988 *Ferromagnetic Materials* vol 11, ed E P Wohlfarth and K H J Buschow (Amsterdam: Elsevier) p 415 and references therein
[2] Peron M N *et al* 1993 *J. Alloys Compounds* **201** 203
[3] Schobinger-Papamantellos P and Buschow K H J 1992 *J. Alloys Compounds* **185** 51
[4] Schobinger-Papamantellos P and Buschow K H J 1991 *J. Less Common Met.* **171** 321
[5] Schobinger-Papamantellos P, Ritter C and Buschow K H J 1998 *J. Alloys Compounds* **264** 89
[6] Schobinger-Papamantellos P, Fauth F and Buschow K H J 1997 *J. Alloys Compounds* **252** 50
[7] Schobinger-Papamantellos P, Buschow K H J, Wilkinson C, Fauth F and Ritter C 1998 *J. Magn. Magn. Mater.* **189** 214
[8] Mun E D, Kwon Y S and Jung M H 2003 *Phys. Rev.* B **67** 033103
[9] Nagarajan R, Patil S, Gupta L C and Vijayaraghavan R 1986 *J. Magn. Magn. Mater.* **54–57** 349
[10] Kaczorowski D 1996 *Solid State Commun.* **99** 949
[11] Das A, Paranjpe S K, Raj P, Satyamoorthy A, Shashikala K and Malik S K 2000 *Solid State Commun.* **114** 87
[12] Taniguchi T, Morimoto H, Miyako Y and Ramakrishnan S 1998 *J. Magn. Magn. Mater.* **177–181** 55
[13] Sato N, Kagawa M, Tanaka K, Takeda N and Komatsubara T 1992 *J. Magn. Magn. Mater.* **104** 31
[14] Bodak O I and Gladyskevskii E I 1969 *Kristallografiya* **14** 990 (in Russian)
[15] Konczyk J, Demchenko P, Matvijishyn R, Pavlyuk V and Marciniak B 2006 *Acta Crystallogr.* E **62** i4
[16] Desclaux J P and Freeman A J 1978 *J. Magn. Magn. Mater.* **8** 119
[17] Barabash S V and Stroud D 2001 *Appl. Phys. Lett.* **7** 979
[18] Kadowaki K and Woods S B 1986 *Solid State Commun.* **58** 507
[19] Potzel W, Kalvius G M and Gal J 1993 *Handbook on the Physics and Chemistry of Rare Earths* vol 17, ed K A Gschneidner Jr, L Eyring, G H Lander and G R Chopin (Amsterdam: Elsevier) p 539
[20] Dunlap B D and Lander G H 1974 *Phys. Rev. Lett.* **33** 1046
[21] Gil A, Szytula A, Tomkowicz Z, Wojciechowski K and Zygmunt A 1994 *J. Magn. Magn. Mater.* **129** 271
[22] Amoretti G 1984 *J. Physique* **45** 1067
[23] Perkins N B, Núñez-Regueiro M D, Coqblin B and Iglesias J R 2007 *Phys. Rev.* B **76** 125101